Autonomous UAV Mission Cycling: A Mobile Hub Approach for Precise Landings and Continuous Operations in Challenging Environments

Alexander Moortgat-Pick, Marie Schwahn, Anna Adamczyk, Daniel A Duecker, Sami Haddadin

***Abstract*— Environmental monitoring via UAVs offers unprecedented aerial observation capabilities. However, the limited flight durations of typical multirotors and the demands on human attention in outdoor missions call for more autonomous solutions. Addressing the specific challenges of precise UAV landings – especially amidst wind disturbances, obstacles, and unreliable global localization – we introduce a mobile hub concept. This hub facilitates continuous mission cycling for unmodified off-the-shelf UAVs. Our approach centers on a small landing platform affixed to a robotic arm, adeptly correcting UAV pose errors in windy conditions. Compact enough for installation in an economy car, the system emphasizes two novel strategies. Firstly, external visual tracking of the UAV informs the landing controls for both the drone and the robotic arm. The arm compensates for UAV positioning errors and aligns the platform's attitude with the UAV for stable landings, even on small platforms under windy conditions. Secondly, the robotic arm can transport the UAV inside the hub, perform maintenance tasks like battery replacements, and then facilitate direct relaunches. Importantly, our design places all operational responsibility on the hub, ensuring the UAV remains unaltered. This ensures broad compatibility with standard UAVs, only necessitating an API for attitude setpoints. Experimental results underscore the efficiency of our model, achieving safe landings with minimal errors ($\leq$ 7 cm) in winds up to 5 Beaufort (8.1 m/s). In essence, our mobile hub concept significantly boosts UAV mission availability, allowing for autonomous operations even under challenging conditions.**

I. Introduction

A. Motivation

Automated deployment of small UAVs from mobile hubs, like passenger cars, offers a significant advancement for extensive environmental monitoring. These hubs facilitate UAV take-off, landing, maintenance, and storage, reducing the manual and cognitive effort of field operations. By deploying multiple UAVs, the hub ensures continuous missions beyond the battery limitations of a single UAV.

This approach streamlines access to UAV monitoring for groups like life science researchers and environmental agencies. They benefit from efficient mission planning and the flexibility to adjust data collection based on changing environmental factors, equipment status, or unforeseen events.

All authors are with Munich Institute of Robotics and Machine Intelligence (MIRMI), Technical University of Munich (TUM), Germany. Contact: author@tum.de

*S. Haddadin has a potential conflict of interest, being a shareholder of Franka Emika GmbH.

The authors would like to thank the Dobeneck Technology Foundation for financial support as part of the SVAN: Synchronous Team-Robot Van project. The authors acknowledge the financial support by the Federal Ministry of Education and Research of Germany (BMBF) in the programme of "Souverän. Digital. Vernetzt." Joint project 6G-life, project identification number 16KISK002.

Fig. 1: Concept of mobile hub enabling continuous UAV missions via a robotic arm providing start, landing, maintenance and storage services from inside a vehicle. Off-the-shelf UAVs are able to autonomously start and land on the platform held by the arm at windspeeds up to 5 Beaufort. Between start and landing, the robotic arm can detach the platform and maintain the UAVs.

With advancements in telepresence systems, experts can now manage mission planning and real-time adaptations remotely [1].

In aerial operations, landing is typically the most safety-critical phase, especially amid wind gusts and confined, obstacle-ridden areas. Often, this landing phase is the main risk determinant, potentially deeming a mission too hazardous. This can lead to mission postponements, even if regular flight is well within the UAV's capabilities. Implementing a hub with an active landing support system, capable of counteracting wind disturbances, can heighten safety and enable autonomous operation in conditions unfavorable for passive systems.

Many landing techniques, especially those paired with UAV base stations and storage, have been examined. Given our focus on the mobile hub, we prioritize techniques apt for vertical take-off and landing (VTOL) vehicles, emphasizing multi-copter systems. These UAVs, needing minimal ground space, fit seamlessly into mobile hub requirements. Direct flight into hub storage might seem straightforward, but it's too perilous. Controlled flight into tensioned nets is common for safe UAV landings, but automated continuation is tough due to the need for manual drone removal. Landing on specific platforms offers a precision-demanding alternative, with the benefit of easily moving the UAV inside for storage or takeoff.

Yet, autonomous UAV landing is fraught with challenges. For secure landings, precise, quick localization near the land-

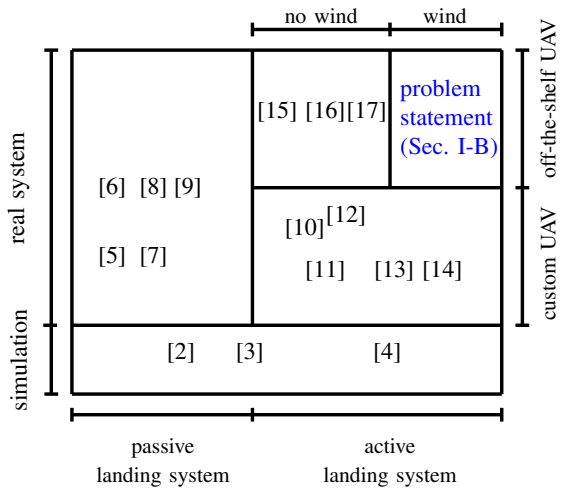

Fig. 2: Comparative analysis of the state of the art in autonomous UAV landing considering the problem statement in I-B. Placement within the blocks is mostly according to publication date, i.e. earlier to latest from left to right, and has no indication of quality or importance of the work.

ing zone is crucial. Solely depending on global navigation satellite systems (GNSS) or even RTK-GPS isn't ideal given their location-dependent accuracy. While UAVs with built-in high-precision localization and advanced controllers would be optimal, most lack these features. A viable alternative is to utilize control APIs of standard UAVs via a wireless link, supplementing them with external localization, such as vision-based systems, and strategies to adjust for positional errors during landing. Our work delves into this solution.

B. Problem Statement

Consider the scenario of deploying an UAV for environmental monitoring from an automatized mobile hub, e. g. a passenger car, with UAV experts only available remotely. Furthermore the hub and the UAV are subject to unexpected wind gusts. Hence, the critical flight phases such as take-off and landing require handling by the mobile hub infrastructure. While high-precision guidance, navigation, and control is required in the vicinity of the mobile hub, robust and safe take-off and landing operations must be performed without hardware modifications or additional computation on the UAV-side.

II. Related Work

The challenge in the proposed concept is autonomous precise landing. Research into UAV autonomous landing began in the early 2000s with small remote-controlled helicopters. The rise of multirotor UAVs has amplified interest in this field. In the following, we review existing work with respect to our problem statement in Sec. I-B.

UAV landings are categorized as passive or active. Passive systems let the UAV handle all landing tasks, often used for moving platforms like vehicles or ships. Active systems involve secondary robots like manipulators, enhancing landing robustness, ideal for indoor missions or disaster responses.

Landing a small helicopter on a robot-mounted platform was simulated in 2006 [2]. In 2011, studies [5] and [6] delved into passive landing systems for UAVs landing on passive moving platforms. Techniques like image-based visual servoing and onboard sensing were proposed by [15] and [8]. Reinforcement learning for UAV landing control was introduced in [13]. Meanwhile, [7] provided a comparison of model predictive control (MPC) for UAV landing. [4] presented a strategy for landing on moving cars, detailing phases like search, landing, and homing. In [9], a boundary layer sliding controller combined with model predictive control is used to handle UAV landings amidst wind disturbances. Ship-based UAV landings using visual tracking and guidance markers are explored in [17]. The concept of landing UAVs on mobile manipulators is theoretically analyzed and simulated in [3]. [11] showcases an automatic UAV docking system using magnets and infrared camera tracking. A coordinated control strategy for UAV landing on a manipulator arm is detailed in [10] and extended for heavier UAVs in [12]. [16] presents a magnetic docking device for UAVs on a manipulator mounted to a UGV, tested indoors. Finally, a commercial solution using a robotic arm for eVTOL UAV deployment is offered by [14].

For clarity, we've provided a structured overview of pertinent literature on autonomous UAV landing in relation to our problem statement in Fig. 2. Our solution must accommodate *unmodified* commercial UAVs in outdoor scenarios, ensuring robust landings even under moderate winds, not just in calm settings. Given the constraints, such as using a typical passenger car as the mobile hub with limited openings, precision during landing becomes crucial. Standard commercial UAV controllers haven't displayed the required precision for direct entry into such mobile hubs outdoors. Therefore, an active landing system, possibly utilizing a robotic arm to offset UAV positioning errors, appears more fitting. While several studies opt for active landing systems, many involve customized or altered commercial UAVs, for instance, by adding magnetic docking mechanisms. Such adaptations make these methods ill-suited for our objective of utilizing off-the-shelf UAVs. Among the strategies applicable to unaltered commercial UAVs, none have proven resilient to wind disturbances during landing. Consequently, we spot a research void for active autonomous landing systems adept in windy conditions without necessitating UAV modifications.

III. Contribution

This work offers a three-pronged contribution:

1) We introduce an automated UAV mission cycling system tailored for mobile drone hubs utilizing standard UAVs as shown in Fig. 3. Central to this is a tactile robot manipulator that dynamically positions a take-off and landing platform, ensuring safe operations even in windy scenarios.
2) Our system design is characterized by three levels of redundant safety measures to enhance error tolerance.
3) Through diverse wind-condition experiments, we assess our strategy, dissecting the quantitative outcomes and highlighting constraints.

In summary, we posit:

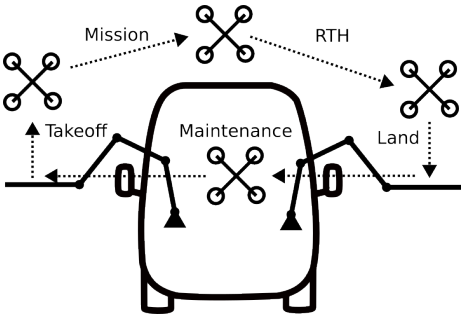

Fig. 3: Autonomous UAV mission cycling based on an automobile equipped with an robotic arm allows to perform takeoff, mission, return to home, landing and maintenance without human input.

(1) Actuating the platform in a horizontal direction can significantly reduce its size.
(2) UAV mishaps can be curtailed by actively synchronizing the platform to the UAV's pitch and roll.
(3) The landing system is feasible within the spatial confines of a typical passenger car, notably its door windows.

IV. Methodology

A. Concept

Our autonomous platform for UAV launch and landing, shown in Fig. 1, facilitates the operation of small UAVs from confined spaces like automobiles. This active landing system eliminates the need for special UAV onboard processing. The UAV simply needs online control input capability, such as desired thrust or roll, pitch, and yaw angles. Instead, a tactile serial manipulator extends from the hub, providing a moving landing platform for the UAV, ensuring safe landing even in windy conditions. Beside usage for UAV maintenance and storage, integrating a robotic arm delivers three main benefits: compensation for UAV landing errors, adjustment for hub tilt due to uneven terrain, and a tactile landing detection system that supplements the UAV's own reporting and visual checks.

For stable landings in windy conditions, the platform tilts against the wind, leveraging the manipulator's speed to correct the UAV's positioning and preventing it from being swept away post-landing. Near the mobile hub, a camera localizes the UAV, ensuring GNSS-independence. The robotic arm's platform adjustment accommodates uneven terrains, like sloped parking. The hub's orientation, denoted as ${}^{\mathcal{G}}R_{\mathcal{S}}$, is determined using an IMU attached to the hub.

The system offers triple redundancy for landing position accuracy: First, the drone maintains its position over the platform. Second, the manipulator positions the platform under the UAV and syncs its orientation. Lastly, a platform size exceeding half of the UAV's diameter plus the typical error margin enhances safety.

Consider the following frames: the global inertial frame $\mathcal{G}$, the stationary frame $\mathcal{S}$ attached to the base station, the manipulator's base frame $\mathcal{O}$, and the end effector frame $\mathcal{E}$. Additionally, we have the platform frame $\mathcal{P}$, camera frame $\mathcal{C}$, vehicle inertial frame $\mathcal{V}$, and UAV body frame $\mathcal{B}$. When

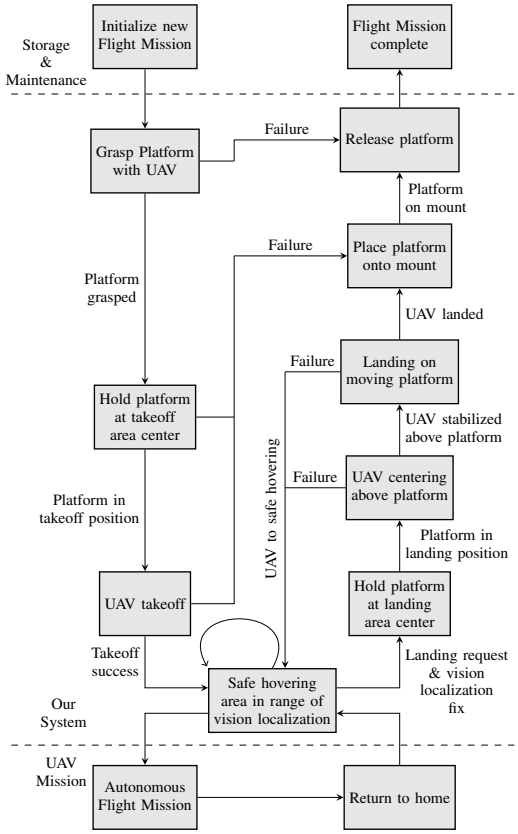

Fig. 4: The proposed strategy for UAV flight missions from a hub involves: (1) The manipulator positioning the UAV atop the platform in a take-off area, (2) UAV take-off and navigation to a safe hovering area using redundant localization, (3) UAV initiation of an autonomous mission or teleoperation, (4) Post-mission UAV return to hovering for localization, (5) Manipulator aligning the landing platform beneath the UAV, (6) Dynamic adjustments to the platform by the manipulator for landing, and (7) UAV storage by placing the platform onto a mount.

the UAV is operational and the hub is static, we have:

$$ {}^{\mathcal{G}}T_{\mathcal{S}}, {}^{\mathcal{S}}T_{\mathcal{O}}, {}^{\mathcal{S}}T_{\mathcal{C}}, {}^{\mathcal{E}}T_{\mathcal{P}} = \text{const.} \tag{1} $$

The manipulator's position, ${}^{\mathcal{S}}T_{\mathcal{O}}$, is determined via a camera identifying a fiducial marker on the static end effector. For the system's moving components, including the UAV, end effector, and platform, the following applies:

$$ {}^{\mathcal{S}}T_{\mathcal{V}}, {}^{\mathcal{V}}T_{\mathcal{B}}, {}^{\mathcal{O}}T_{\mathcal{E}} \neq \text{const.} \tag{2} $$

The pivotal frame $\mathcal{S}$ links the entire system: camera-based localization, UAV, and manipulator. The challenge is to localize the UAV within $\mathcal{S}$ and adeptly control both UAV and manipulator in $\mathcal{S}$.

B. UAV Mission Cycling Strategy

Our system offers an autonomous bridge between a stored UAV and its flight mission, enabling repeated cycles. This procedure is illustrated in Fig. 4.

Initially, a fully-charged UAV rests on the platform inside storage. The manipulator retrieves it, positioning it centrally in the external take-off zone (refer to Fig. 1 bottom). Post-arrival, a take-off command propels the UAV, which is

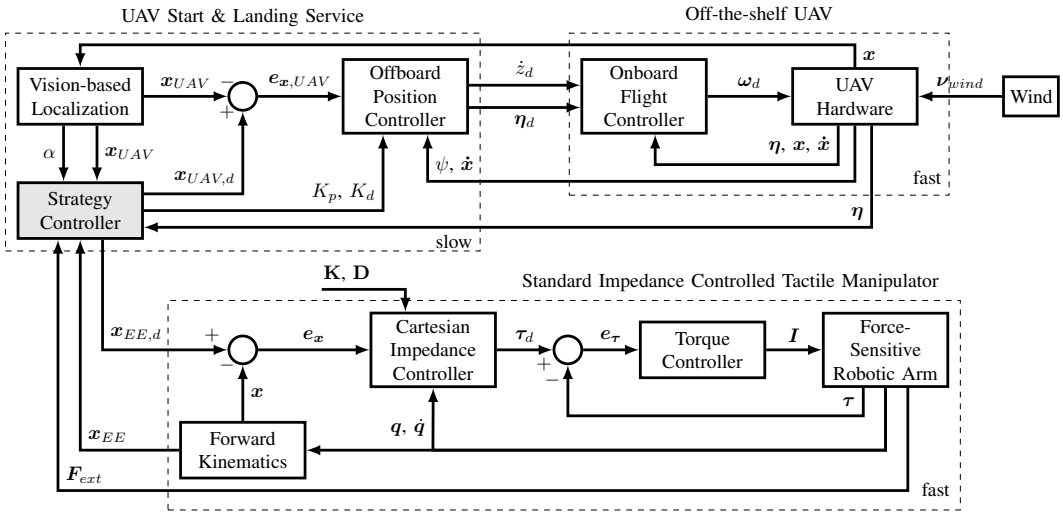

Fig. 5: The control scheme comprises: the UAV start and landing system (*top left*), the UAV's onboard controller (*top right*), and an impedance-controlled tactile manipulator (*bottom*). The service discerns UAV position $\boldsymbol{x}UAV$ through a fiducial marker. The strategy controller, limited by vision, determines the desired UAV pose $\boldsymbol{x}UAV, d$, sets gains K_p and K_d via flag α, and specifies the manipulator end effector's target pose $\boldsymbol{x}EE, d$. Feedback on end effector pose $\boldsymbol{x}EE$, external wrench $\boldsymbol{F}ext$, UAV attitude $\boldsymbol{\eta}$, and position $\boldsymbol{x}UAV$ guides the strategy controller's transitions as per Fig. 4.

promptly directed to a safe hovering position, leveraging dual localization via the hub's computer vision and GNSS.

In the safe hover zone, the UAV awaits either an autonomous mission signal or teleoperated control. This zone ensures UAVs hover without obstacle collision, even if one localization method (GNSS or vision) fails, acting as a safety net against flight control malfunctions.

Post-mission, off-the-shelf UAVs leverage GNSS for 'return home'. Upon its return, the system activates a landing sequence once visual localization is secured. The manipulator situates the platform at the landing zone's center, after which the UAV stabilizes directly above it.

Landing for standard UAVs is innate; a trigger initiates a descent using onboard sensors. Our strategy integrates with this, ensuring platform movement doesn't confuse the UAV. If the platform shifts during UAV stabilization, the UAV might misinterpret the movement. To counteract, our method only shifts the platform after initiating landing, and it moves both horizontally and vertically, minimizing UAV's positional errors. Moreover, the manipulator synchronizes the platform's orientation with the UAV's attitude, making frames $\mathcal{P}$ and $\mathcal{B}$ parallel, enhancing landing reliability (elaborated in Section V and displayed in Fig. 9).

After a successful landing, the manipulator returns the platform and UAV to storage. This completes one mission cycle, readying the UAV for its next task. Our strategy controller (see Fig. 5) can identify and rectify botched landings using feedback. In failure scenarios, the UAV is guided back to the hover zone. Given the intricacy of the landing phase, our subsequent analysis emphasizes the landing strategy's control, execution, and assessment.

C. Control Scheme

We now introduce the landing strategy's control scheme depicted in Fig. 5. A crucial aspect is localizing the UAV in the frame $\mathcal{S}$. We employ a fiducial marker detection method via a camera feed, specifically using an AprilTag [18], to determine the UAV's position $\boldsymbol{x}_{\text{uav}} = [x, y, z]^T$ based on the marker's position relative to the camera frame. We directly source the yaw angle ${}^{\mathcal{V}}\psi$ and velocity ${}^{\mathcal{V}}\dot{\boldsymbol{x}}$ from the UAV's onboard sensors, circumventing marker detection issues due to perspective ambiguity, especially with distant markers or small image sizes. Alternative localization techniques, like laser or model-based visual tracking, can determine $\boldsymbol{x}_{\text{UAV}}$ without relying on the UAV's sensors.

Our initial studies indicated that even a rudimentary PD control scheme suffices to command off-the-shelf UAVs. This can be expressed as:

$$\boldsymbol{\eta}_d = \boldsymbol{K}_{p,\eta}(\boldsymbol{x}_d - \boldsymbol{x}) + \boldsymbol{K}_{d,\eta}(\dot{\boldsymbol{x}}_{\boldsymbol{d}} - \dot{\boldsymbol{x}}), \tag{3}$$

$$\dot{x}_{z,d} = K_{p,z}(x_{z,d} - x_z) + K_{d,z}(\dot{x}_{z,d} - \dot{x}_z), \tag{4}$$

where $\boldsymbol{\eta}_d = [\phi_d, \theta_d, \psi_d]^T$ represents the UAV's desired orientation in frame $\mathcal{V}$, and $\boldsymbol{x}_d$ and $\dot{\boldsymbol{x}}_d$ denote the desired position and velocity, respectively. The terms $\boldsymbol{K}_{p,\eta}$ and $\boldsymbol{K}_{d,\eta}$ are the proportional and derivative gains for attitude, while $K_{p,z}$ and $K_{d,z}$ pertain to altitude.

Although this method is less sophisticated than, for instance, Model Predictive Control (MPC) in terms of positioning accuracy and stability against disturbances, our system is designed for plug-and-play functionality with standard UAVs, eliminating the need for intricate UAV modeling. This underscores the efficacy of our approach even with such basic UAV controls.

The redundant serial manipulator with flexible joints can be modelled as [19]

$$\mathbf{M}(\boldsymbol{q})\ddot{\boldsymbol{q}} + \mathbf{C}(\boldsymbol{q}, \dot{\boldsymbol{q}})\dot{\boldsymbol{q}} + \boldsymbol{g}(\boldsymbol{q}) = \mathbf{K}(\boldsymbol{\theta} - \boldsymbol{q}) + \boldsymbol{\tau}_{ext} \tag{5}$$

$$\mathbf{B}\ddot{\boldsymbol{\theta}} + \mathbf{K}(\boldsymbol{\theta} - \boldsymbol{q}) = \boldsymbol{\tau}_m, \tag{6}$$

where $\boldsymbol{q} \in \mathbb{R}^7$ are the link and $\boldsymbol{\theta} \in \mathbb{R}^7$ the motor positions, $\mathbf{M}(\boldsymbol{q}) \in \mathbb{R}^{7x7}$ is the inertia matrix, $\mathbf{C}(\boldsymbol{q}, \dot{\boldsymbol{q}})\dot{\boldsymbol{q}} \in \mathbb{R}^{7x7}$ the centripetal and Coriolis vector. Furthermore, $\boldsymbol{g}(\boldsymbol{q}) \in \mathbb{R}^7$

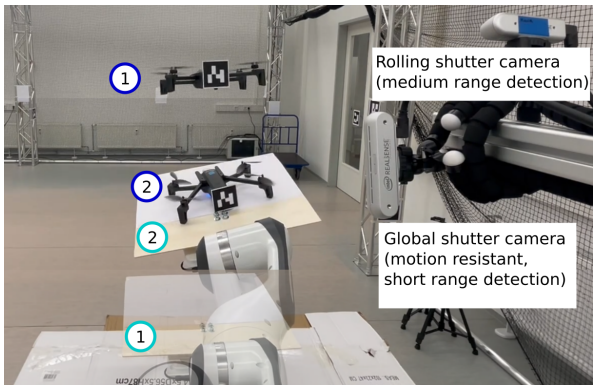

Fig. 6: The fiducial marker on the UAV's rear facilitates vision-based localization. During landing, the UAV maintains a fixed position above the manipulator's workspace outside the hub. After stabilizing its position (1), the UAV initiates the landing procedure. Concurrently, the manipulator aligns the platform's center with the UAV's center of mass in the inertial frame $\mathcal{G}$, ensuring the platform is parallel to the UAV's body frame $\mathcal{B}$ (2).

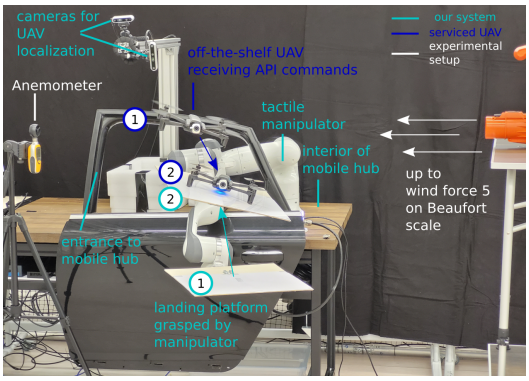

Fig. 7: We conducted a series of experiments to test the landing under controlled conditions. Two cameras served to as external positioning system for the UAV. Wind was created with a leafblower aimed at the UAV during stabilization and landing. The wind speed was measured with an anemometer.

denotes the gravity vector, $\mathbf{K}$ and $\mathbf{B}$ are the joint stiffness and motor inertia matrices, $\boldsymbol{\tau}_m$ is the motor torque vector, and $\boldsymbol{\tau}_{ext}$ the vector of external forces acting on the end-effector by the environment.

We use a standard Cartesian impedance controller in order to achieve compliant behavior in case of contact as well as for the added benefit that individual DOFs can be relaxed by lowering the corresponding stiffness value. The closed loop dynamics for the impedance controller read

$$\boldsymbol{\Lambda}(\boldsymbol{q})\ddot{\boldsymbol{e}}_x + \mathbf{D}_d\dot{\boldsymbol{e}} + \mathbf{K}_d\boldsymbol{e}_x + \bar{\mathbf{C}}(\boldsymbol{q},\dot{\boldsymbol{q}})\dot{\boldsymbol{e}}_x = \mathbf{F}_{ext}. \quad (7)$$

Here, $\boldsymbol{\Lambda}(\boldsymbol{q}) = (\mathbf{J}(\boldsymbol{q})\bar{\mathbf{M}}(\boldsymbol{q})^{-1}\mathbf{J}(\boldsymbol{q})^T)^{-1}$ denotes the equivalent Cartesian mass matrix with $\mathbf{J}(\boldsymbol{q})$ being the Jacobian. The desired damping and stiffness matrices are denoted by $\mathbf{D}_d$ and $\mathbf{K}_d$, respectively. Moreover, $\bar{\mathbf{C}}(\boldsymbol{q},\dot{\boldsymbol{q}})$ is an arbitrary skew symmetric matrix and $\boldsymbol{e}_x = \boldsymbol{x}_d - \boldsymbol{x}$ represents the control error. The estimated external force acting on the end effector $\mathbf{F}_{ext}$ is fed back to the strategy controller. It contains the contact force between UAV and platform which can be used for additional redundant landing and error state detection.

The control loops for the UAV and manipulator operate independently, as depicted in Fig. 5. We refrained from adopting a cooperative control approach, where the UAV would consider the platform's position, for several reasons: (1) The manipulator has notably superior positioning accuracy and quicker dynamics compared to typical UAVs which adjust position using air displacement; (2) UAV localization inaccuracies introduce considerable delays into both robots' control loops; (3) The wireless nature of communication with the UAV adds extra delays, complicating synchronous control with the manipulator; and (4) Manipulator-based errors, such as torque or joint limit violations, are more effectively addressed by the strategy controller rather than through UAV compensations.

D. Implementation

In this study, we developed a prototype utilizing a Franka Emika Research 3 (FE3) serial manipulator [20], supplemented with two Intel NUC computers and two Intel Realsense cameras (D435i and D455). The D455 with its global shutter provides higher tracking robustness at a shorter effective range. A custom 3D-printed handle, designed to fit the FE3's fingers, attaches to a 0.4 m side-length plywood platform. Our experiments employed the Parrot Anafi UAV [21], although our method is adaptable to various commercial UAVs. The software infrastructure is anchored on ROS noetic [22] running on Ubuntu 20.04.

One computer, equipped with a realtime-patched kernel, manages the Cartesian impedance controller for the FE3 through the 'franka_ros' ROS package, also overseeing a joint position controller for select strategy tasks. The secondary computer orchestrates the strategy controller, vision localization, and UAV offboard position control. The Parrot Anafi UAV integrates with our setup through the Parrot Olympe SDK, a Python toolset compatible with Ubuntu 20.04 and embeddable within a ROS node. This UAV offers a live video stream enriched with metadata detailing UAV state parameters. For UAV localization, the 'aruco-ros' ROS package pinpoints fiducial marker positions, integrating seamlessly with the AprilTag [18] library. The overarching strategy controller operates as a ROS node, synchronizing data across the manipulator, vision localization, and UAV, while managing state transitions via ROS service calls.

V. Experiments

A. Experimental Setup

We conducted three experiments under identical windy conditions to assess claims 1 and 2 from Sec. III, using the prototype detailed in Sec. IV-D. In-lab wind, simulating wind force 5 on the Beaufort scale with an average velocity of $8.1\frac{m}{s}$, was generated using a leaf blower aimed at the UAV.

Experiment 1, serving as a reference, utilized the system's full proposed functionality with a moving and attitude-aligned platform. Experiment 2 tested UAV landing on a flat surface using external vision-based localization. Experiment 3 examined landing on a manipulator-moved platform without attitude-alignment to discern its advantages.

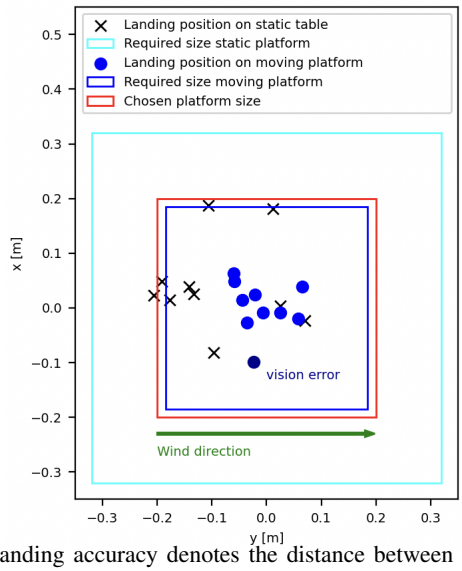

Fig. 8: Landing accuracy denotes the distance between the UAV's center of mass upon landing and the platform's center. The platform's requisite size combines the maximal error under acceptable wind conditions, half the UAV's diameter, and a safety margin. Our dynamic platform approach considerably minimizes the needed platform size in windy scenarios.

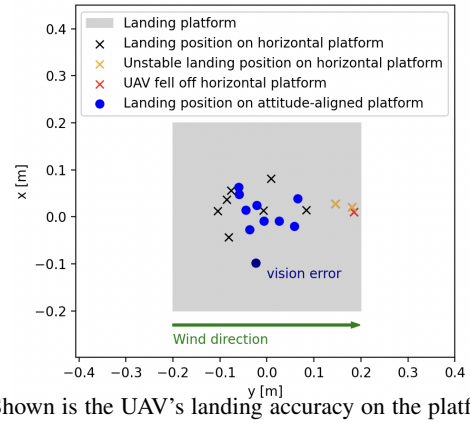

Fig. 9: Shown is the UAV's landing accuracy on the platform under windy conditions: without platform alignment (cross) and with platform alignment to UAV's attitude (point). Absence of attitude-alignment resulted in one UAV fall-off (red ×) and two near fall-offs (orange ×). Attitude-alignment consistently yields tighter landing position groupings in windy situations.

For each test, we recorded landing accuracy as the distance between the UAV's landed center of mass and the platform's midpoint.

B. Results

1) Platform size reduction by platform alignment: Figure 8 showcases results from experiments 1 and 2, examining claim 1 about reducing landing platform size as outlined in Sec. III. Considering the UAV's 24 cm span and experiment 1's landing accuracy, a static landing platform requires 64 cm x 64 cm. This can be decreased by 27 cm to 37 cm x 37 cm with a dynamically aligned platform. Thus, the suggested platform size for our system is 40 cm x 40 cm.

2) Prevent UAV falling off by dynamic orientation alignment: Figure 9 presents results from experiments 1 and 3, evaluating claim 2 regarding the system's ability to keep the

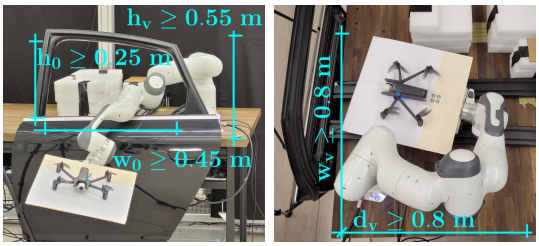

(a) Vehicle side view. (b) Vehicle top view.

Fig. 10: Shown are the required minimal dimensions of the system setup within a vehicle for a chosen platform size of 40 cm x 40 cm. The opening is defined by the width w_o and height h_o and the interior of the vehicle by width w_v and depth d_v.

UAV stable on the platform post-landing in windy scenarios, as discussed in III. In experiment 3, the UAV fell off the 40 cm x 40 cm platform once and nearly toppled in two instances. However, when the platform's orientation aligns with the UAV's body frame upon contact, the UAV consistently landed stably. This alignment, influenced by the wind and indicated by the UAV's in-flight attitude, effectively ensures the UAV's stability on the landing platform.

3) System Composition Suitability for Vehicle Integration: To evaluate claim 3, we examine the system configuration using a 40 cm x 40 cm platform, as shown in Fig. 10. This configuration informs the minimal vehicle dimensions ensuring collision-free UAV transportation in and out. The vehicle's entryway should exceed a 0.45 m width and 0.25 m height to accommodate links 6 and 7 of the manipulator. Internally, the minimal width and depth are 0.8 m each, with an ideal height surpassing 0.55 m for the manipulator's optimal arrangement (Fig. 10b). Consequently, vehicles from the compact class upwards can accommodate the system.

VI. Conclusion

In this study, we addressed the challenge of autonomous UAV mission cycling, encompassing active take-off, mission, return to home, landing, and maintenance or storage. A primary criterion was the system's compatibility with standard UAVs – no hardware changes – whilst ensuring reliable landings amidst wind disturbances. Drawing from comprehensive literature, we introduced an innovative landing system, leveraging a tactile manipulator to centrally position a landing platform beneath the UAV. This platform also aligns with the UAV's attitude, ensuring stability post-landing in windy settings.

Our experiments showcased the efficacy of this strategy: consistent landings with minimal errors (under 7 cm) even at wind speeds reaching 5 Beaufort (8.1 m/s). This technique enhances UAV mission readiness by facilitating autonomous operations from mobile hubs in challenging wind conditions.

Going forward, we'll delve into the platform's ground effect on the UAV and strategies to mitigate it. Additionally, we'll compare various control schemes to understand the system's constraints and conduct extensive outdoor tests to validate its real-world applicability.

REFERENCES

[1] A. Moortgat-Pick, P. So, M. J. Sack, E. G. Cunningham, B. P. Hughes, A. Adamczyk, A. Sarabakha, L. Takayama, and S. Haddadin, "A-rift: Visual substitution of force feedback for a zero-cost interface in telemanipulation," in *2022 IEEE/RSJ International Conference on Intelligent Robots and Systems (IROS)*. IEEE, 2022, pp. 3926–3933.

[2] K. Dalamagkidis, S. Ioannou, K. Valavanis, and E. Stefanakos, "A mobile landing platform for miniature vertical take-off and landing vehicles," in *2006 14th Mediterranean Conference on Control and Automation*. IEEE, 2006, pp. 1–6.

[3] V. Lippiello, R. Mebarki, and F. Ruggiero, "Visual coordinated landing of a uav on a mobile robot manipulator," in *2013 IEEE International Symposium on Safety, Security, and Rescue Robotics (SSRR)*. IEEE, 2013, pp. 1–7.

[4] J. Ghommam and M. Saad, "Autonomous landing of a quadrotor on a moving platform," *IEEE Transactions on Aerospace and Electronic Systems*, vol. 53, no. 3, pp. 1504–1519, 2017.

[5] K. E. Wenzel, A. Masselli, and A. Zell, "Automatic take off, tracking and landing of a miniature uav on a moving carrier vehicle," *Journal of intelligent & robotic systems*, vol. 61, pp. 221–238, 2011.

[6] B. Herissé, T. Hamel, R. Mahony, and F.-X. Russotto, "Landing a vtol unmanned aerial vehicle on a moving platform using optical flow," *IEEE Transactions on robotics*, vol. 28, no. 1, pp. 77–89, 2011.

[7] J. A. Macés-Hernández, F. Defaÿ, and C. Chauffaut, "Autonomous landing of an uav on a moving platform using model predictive control," in *2017 11th Asian Control Conference (ASCC)*. IEEE, 2017, pp. 2298–2303.

[8] D. Falanga, A. Zanchettin, A. Simovic, J. Delmerico, and D. Scaramuzza, "Vision-based autonomous quadrotor landing on a moving platform," in *2017 IEEE International Symposium on Safety, Security and Rescue Robotics (SSRR)*. IEEE, 2017, pp. 200–207.

[9] A. Paris, B. T. Lopez, and J. P. How, "Dynamic landing of an autonomous quadrotor on a moving platform in turbulent wind conditions," in *2020 IEEE International Conference on Robotics and Automation (ICRA)*. IEEE, 2020, pp. 9577–9583.

[10] M. Maier and K. Kondak, "Landing of vtol uavs using a stationary robot manipulator: A new approach for coordinated control," in *2015 54th IEEE Conference on Decision and Control (CDC)*. IEEE, 2015, pp. 1497–1502.

[11] W.-C. Lu and W.-S. Wang, "Design of an automatic docking system for quadcopters," in *2016 Asia-Pacific Conference on Intelligent Robot Systems (ACIRS)*. IEEE, 2016, pp. 199–203.

[12] M. Maier, K. Kondak, and C. Ott, "Enabling robot assisted landing of heavy uav rotorcraft via combined control and workload sharing," in *2017 IEEE/RSJ International Conference on Intelligent Robots and Systems (IROS)*. IEEE, 2017, pp. 5128–5134.

[13] A. Rodriguez-Ramos, C. Sampedro, H. Bavle, I. G. Moreno, and P. Campoy, "A deep reinforcement learning technique for vision-based autonomous multirotor landing on a moving platform," in *2018 IEEE/RSJ International Conference on Intelligent Robots and Systems (IROS)*. IEEE, 2018, pp. 1010–1017.

[14] Quantum Systems Long-range eVTOL fixed wing UAVs, https://quantum-systems.com/, Accessed: 2023/03/02.

[15] D. Lee, T. Ryan, and H. J. Kim, "Autonomous landing of a vtol uav on a moving platform using image-based visual servoing," in *2012 IEEE international conference on robotics and automation*. IEEE, 2012, pp. 971–976.

[16] E. Narváez, A. A. Ravankar, A. Ravankar, T. Emaru, and Y. Kobayashi, "Autonomous vtol-uav docking system for heterogeneous multirobot team," *IEEE Transactions on Instrumentation and Measurement*, vol. 70, pp. 1–18, 2020.

[17] B. Lee, V. Saj, D. Kalathil, and M. Benedict, "Intelligent vision-based autonomous ship landing of vtol uavs," *Journal of the American Helicopter Society*, 2023.

[18] E. Olson, "Apriltag: A robust and flexible visual fiducial system," in *2011 IEEE international conference on robotics and automation*. IEEE, 2011, pp. 3400–3407.

[19] M. W. Spong, "Modeling and control of elastic joint robots," 1987.

[20] Franka Emika Robot, https://www.franka.de/, Accessed: 2023/03/01.

[21] Parrot Anafi Drone, https://www.parrot.com/en/drones/anafi, Accessed: 2023/03/02.

[22] M. Quigley, K. Conley, B. Gerkey, J. Faust, T. Foote, J. Leibs, R. Wheeler, and A. Y. Ng, "Ros: an open-source robot operating system," in *ICRA workshop on open source software*, vol. 3, no. 3.2. Kobe, Japan, 2009, p. 5.